

Hot Dense Matter and Stellar Collapse

D. Q. Lamb, J. M. Lattimer, C. J. Pethick,^(a) and D. G. Ravenhall

*Department of Astronomy and Department of Physics, University of Illinois at Urbana-Champaign,
Urbana, Illinois 61801*

(Received 17 October 1978)

We calculate the equation of state for hot dense matter and discuss implications for stellar collapse.

A reliable equation of state for matter at temperatures of order 10^{11} K and at densities ranging up to nuclear-matter density is crucial for understanding supernovae and neutron-star formation. Such hot dense matter consists of a mixture of heavy nuclei, α particles, neutrons, protons, electrons, and neutrinos. Among the important physical features that must be incorporated in any consistent treatment of this mixture are the nuclear forces among the nucleons, the effects of temperature and of the external nucleons on the properties of nuclei, and the Coulomb forces between nuclei. Some of these effects have been included in previous calculations.¹⁻³ Here we present a consistent and systematic calculation, based on the compressible-liquid-drop model of the nucleus,⁴ that incorporates all of them. We describe the phase diagram for hot dense matter and discuss the implications for stellar collapse.

We consider the properties of matter in nuclear statistical equilibrium, that is, in equilibrium with respect to strong and electromagnetic interactions, but not necessarily with respect to weak interactions. One finds the equilibrium state by minimizing the free energy of a fixed volume of matter at temperature T , assuming charge neutrality, and keeping the total numbers of neutrons and protons fixed. The state of the nucleons can be determined without reference to the leptons, since the latter can be treated as ideal Fermi gases and therefore their free energy is independent of the configuration of the nucleons.

The presence of nuclei dramatically influences both the equation of state and the mean free path of neutrinos. It is therefore important to determine the ranges of densities and temperatures for which nuclei coexist with an external nucleon gas. The qualitative features of this coexistence are determined primarily by the properties of uniform bulk matter. Lattimer and Ravenhall⁵ have studied this bulk equilibrium using a Skyrme potential to describe the nuclear force.

The resulting phase diagram for bulk matter is shown in Fig. 1 for matter consisting of 25% protons; that is, the number of electrons per nucle-

on, Y_e , is 0.25. This value is typical of those that are of interest in stellar collapse, but the phase diagram is very insensitive to the proton concentration for $0.2 \lesssim Y_e \lesssim 0.5$. Outside the dotted curve, matter consists of a single homogeneous phase, while inside it consists of two phases, having different densities and proton concentrations, which are in equilibrium. With surface and Coulomb effects included, the denser phase is distributed as droplets, i.e., nuclei. Within the two-phase region, the fraction of nucleons in the denser phase increases from zero at the low-density boundary to one at the high-density boundary. Above and to the left of the low-density portion of the boundary, the denser phase evaporates. This part of the boundary is given approximately by the Saha equation with a binding energy of ~ 16 MeV/nucleon for the denser phase. The high-density boundary corresponds to the density at which nuclei touch and then coalesce, and thus occurs at roughly nuclear-matter density $\rho_0 \approx 3 \times 10^{14}$ g cm⁻³. It is independent of temperature because the matter in nuclei is degenerate with a Fermi temperature of ~ 40 MeV. An important conclusion of the bulk equilibrium calculation is that nuclei survive to high

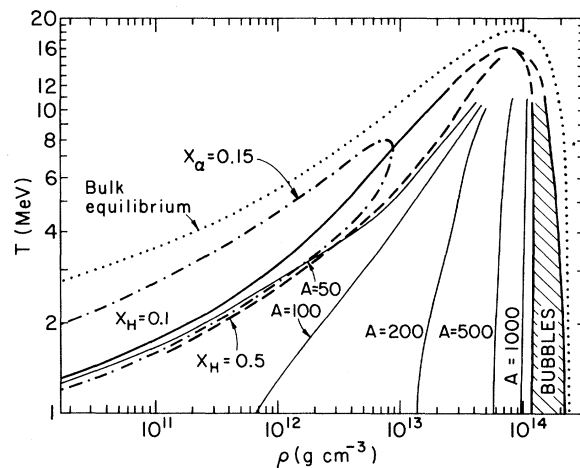


FIG. 1. Composition of hot dense matter for $Y_e = 0.25$. For comparison, the dotted curve shows the boundary of the two-phase region for bulk equilibrium.

temperatures (~ 20 MeV or 2×10^{11} K) at densities approaching ρ_0 . This result is similar to that found by Sato² and is confirmed by the more detailed calculations we describe below.

To extend our treatment to nuclei of finite size, we generalize to finite temperatures the approach of Baym, Bethe, and Pethick⁴ and treat the nuclei as finite drops of compressible nuclear matter surrounded by a sea of nucleons and α particles. The free energy of a nucleus consists of bulk, surface, translational, and Coulomb contributions (including the Coulomb interaction between nuclei). We assume all the nuclei to be identical. For the surface free energy we use results⁶ obtained from a Thomas-Fermi finite-temperature generalization of the approach of Ravenhall, Bennett, and Pethick.⁷ The volume free energies of both the nuclei and the external nucleons and the surface free energy are all computed using the same Skyrme effective nucleon-nucleon interaction, which ensures a consistent treatment of the phases and the interface. Our treatment of the Coulomb free energy follows that of Ref. 4, extended to finite temperatures using the Coulomb liquid calculations of Hansen.⁸ We take the α particles to be an ideal Boltzmann gas, and neglect the effects of the external nucleons on their binding energy.

The resulting composition diagram for hot dense matter is shown in Fig. 1 for $Y_e = 0.25$. In contrast to the situation for bulk equilibrium, there is no definite boundary to the region in which nuclei exist but instead the mass fractions X_H in heavy nuclei, and X_α in α particles vary continuously over the ρ - T plane. We show lines corresponding to $X_H = 0.1$, and to $X_\alpha = 0.15$. As ρ increases, the fraction of space filled by nuclei increases until when it is $\sim \frac{1}{2}$, the nuclei turn inside out, and the density inhomogeneities then consist of "bubbles" of less-dense matter. The high-density boundary of the bubble region shown in Fig. 1 corresponds to $\sim 10^{-3}$ of the matter being in bubbles. The region in which an appreciable fraction of the matter is in nuclei (or bubbles) corresponds rather closely to the two-phase region of the phase diagram for bulk equilibrium, and is relatively insensitive to changes in the proton fraction for $0.2 \lesssim Y_e \lesssim 0.5$. In comparison with bulk matter, the low-density boundary of this region is shifted to lower temperatures since surface and Coulomb effects lower the nuclear binding energy (here ~ 9 MeV/nucleon). At lower temperatures one expects crystallization of nuclei and bubbles, an effect which will be dis-

cussed elsewhere.

Figure 1 also shows the contours of constant mass number A of the equilibrium nucleus. At high temperatures, the free energy of a nucleus is relatively insensitive to its mass number. One then expects a range of nuclei with different masses to be present, and our treatment in terms of a single representative nucleus may require modification. Near the critical temperature of ~ 16 MeV, a spectrum of sizes of both nuclei and bubbles will be present, representing density fluctuations. In this region, our treatment of nuclei in terms of the compressible-liquid-drop model encounters some of the same difficulties faced by the liquid-drop model of gas-liquid phase transitions,⁹ but we expect the resulting uncertainties to have little effect on the conclusions we draw below. The affected portions of various curves are indicated by dashed lines.

Our calculations have important implications for stellar collapse. Consider a collapsing, homogeneous stellar core. For densities in excess of $\sim 10^{12}$ g cm⁻³ the mean free path of neutrinos is so short that they are trapped within the core, so that the total number of leptons per nucleon, Y_l , is conserved in the subsequent collapse. In addition the weak-interaction rates are sufficiently fast that, first, the matter is essentially in β equilibrium, and, second, little entropy is generated. Consequently the trajectory of core is to a good approximation an adiabat corresponding to matter in β equilibrium, and may be parametrized by Y_l and by s , the entropy per baryon in units of Boltzmann's constant. In Fig. 2 we show such adiabats for $Y_l = 0.25$ and 0.35 . The values $s = 1$ to 3 bracket recent calculations. Arnett³ found that $s \approx 2.5$ and $Y_l \approx 0.23$ subsequent to neutrino trapping while Bethe *et al.*¹⁰ have recently suggested that $s \sim 1$ and $Y_l \sim 0.35$. The figure shows the lines corresponding to $X_H = 0.1$ and 0.5 , and lines bounding the bubble region, all of which are little changed by variations of Y_l in the range 0.25 - 0.5 . We also show Arnett's³ collapse trajectory, which terminates in a bounce at $\rho \sim 3 \times 10^{13}$ g cm⁻³. The difference between it and our adiabats for similar values of s and Y_l is due to our consistent treatment of dripped nucleons and nuclei and to the effects of nuclear excited states, which were automatically included in our approach through the temperature dependence of the bulk and surface free energies. We conclude that nuclei persist up to essentially nuclear-matter density along all likely collapse

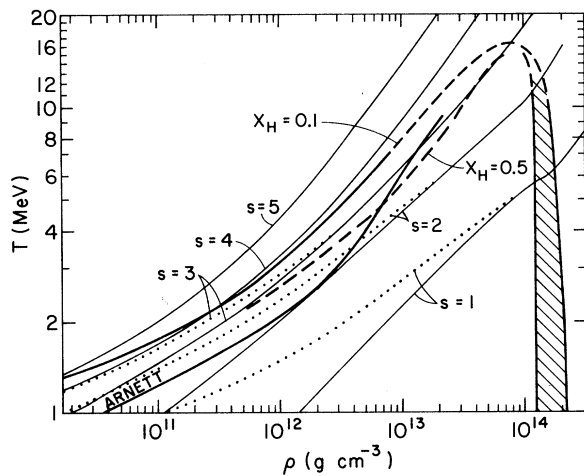


FIG. 2. Adiabats on a T - ρ plot. The thin solid lines are adiabats for $Y_1 = 0.25$. The dotted curves are those for $Y_1 = 0.35$. Also shown are Arnett's trajectory, and some features of the composition diagram (Fig. 1).

trajectories.

A useful measure of the stiffness of matter is the adiabatic index $\Gamma = (\partial \ln P / \partial \ln n)_{s, Y_1}$, where P is the pressure and n is the total baryon density. Nonrelativistically, collapse cannot be halted unless Γ exceeds $\frac{4}{3}$. The effects of general relativity and the momentum of the collapse raise this limit into the range 1.4–1.5.¹¹ In Fig. 3 we display Γ as a function of density along the adiabats for $Y_1 = 0.25$. For large Y_1 , Γ is very close to $\frac{4}{3}$ since the relativistic electrons provide most of the pressure. For small s and large Y_1 , nearly all nucleons are in nuclei, and have little effect on the pressure or on Γ . As s increases or Y_1 decreases, the fraction of nucleons outside nuclei, X_d , increases, and they play an increasingly important role. Γ remains rather close to $\frac{4}{3}$ for $s < 3$, even when X_d is significant, because of the two-phase character of the nucleon system. As the density is increased adiabatically, entropy is transferred from the external nucleons to the nuclear excited states, and consequently the temperature and pressure increase more slowly than they would if the entropy in the external nucleon gas were constant. Thus the pressure of the external nucleons increases less rapidly than it otherwise would, and Γ remains low. At densities below $\sim 10^{13}$ g/cm³, Γ increases with ρ since X_d increases, while at larger densities Γ begins to decrease since X_d decreases. Part of the drop in Γ is due also to the effect of the attractive nucleon-nucleon interaction in the nucleon gas, which can more than compensate for the onset of

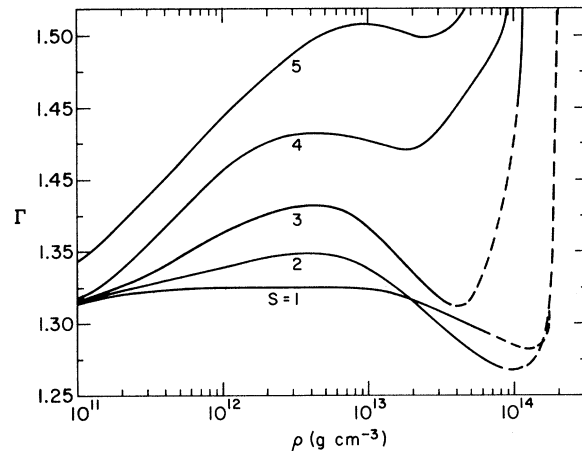


FIG. 3. Adiabatic indices as a function of ρ , for $Y_1 = 0.25$ and for the indicated s values. For simplicity, the curves have been smoothed in the dashed regions to remove some inessential details.

degeneracy. Γ increases sharply and rises above $\frac{4}{3}$ again when the density approaches ρ_0 and the nuclei fill the whole of space. The adiabats $s = 4$ and 5 lie largely outside the region where X_H is appreciable, and for them Γ deviates more from $\frac{4}{3}$.

Our results show that as long as $Y_1 \geq 0.2$ and $s \leq 3$, Γ is less than 1.4 up to densities $\approx 10^{14}$ g/cm³, due essentially to the survival of the nuclei. Thus we conclude that for all stellar-collapse calculations now being considered, *collapse will be halted only at nuclear densities or greater*. An understanding of the bounce itself will require a reliable description of hot matter beyond nuclear densities.

We thank D. Arnett for making available unpublished results of his calculations. We have benefited from discussions with him and also with G. Baym and R. I. Epstein. It is a pleasure to acknowledge the warm hospitality of NORDITA, where part of this research was carried out. One of us (D.Q.L.) gratefully acknowledges support of the John Simon Guggenheim Memorial Foundation, and another (D.G.R.) the support and hospitality of the Centre d'Etudes Nucléaires, Saclay, during 1977–1978. This research was supported in part by National Science Foundation Grants No. AST 76-22673, No. PHY 77-25279, and No. PHY 78-04404.

(a) Also at NORDITA, Copenhagen, Denmark.

¹S. A. Bruenn, W. D. Arnett, and D. N. Schramm, *Astrophys. J.* **213**, 213 (1977); T. J. Mazurek, to be published; T. J. Mazurek, J. M. Lattimer, and C. E. Brown, to be published; J. R. Wilson, in "Proceedings of the International School of Physics 'Enrico Fermi,' Varenna, Italy, 1975" (to be published).

²K. Sato, *Prog. Theor. Phys.* **54**, 1325 (1975).

³W. D. Arnett, *Astrophys. J.* **218**, 815 (1977).

⁴G. Baym, H. A. Bethe, and C. J. Pethick, *Nucl. Phys. A* **175**, 225 (1971).

⁵J. M. Lattimer and D. G. Ravenhall, *Astrophys. J.* **223**, 314 (1978).

⁶D. G. Ravenhall and J. M. Lattimer, to be published.

⁷D. G. Ravenhall, C. D. Bennett, and C. J. Pethick, *Phys. Rev. Lett.* **28**, 978 (1972).

⁸J. P. Hansen, *Phys. Rev. A* **8**, 3096 (1973).

⁹M. E. Fisher, in *Critical Phenomena, Proceedings of the International School of Physics "Enrico Fermi," Course LI*, edited by M. S. Green (Academic, New York, 1971), p. 50.

¹⁰H. A. Bethe, G. E. Brown, J. Applegate, and J. M. Lattimer, to be published.

¹¹K. A. Van Riper and W. D. Arnett, *Astrophys. J.* **225**, L19 (1978); K. A. Van Riper, to be published.

ERRATA

HIGH-RESOLUTION X-RAY STUDY OF A SECOND-ORDER NEMATIC-SMECTIC-A PHASE TRANSITION. J. Als-Nielsen, R. J. Birgeneau, M. Kaplan, J. D. Litster, and C. R. Safinya [*Phys. Rev. Lett.* **39**, 352 (1977)].

In this paper we reported a high-resolution x-ray study of the nematic-smectic-A (*N-A*) transition in *N-p*-cyanobenzylidene-*p*-octyloxyaniline (CBOOA) for reduced temperature $2 \times 10^{-2} \geq \tau = T/T_c - 1 \geq 8 \times 10^{-5}$. For the data closest to T_c the intrinsic longitudinal width was comparable with the instrumental resolution so that accurate numerical deconvolutions were necessary to extract the intrinsic fluctuation spectra. In the work presented in this paper we took the resolution function to be Gaussian in the vertical and longitudinal in-plane directions. The transverse in-plane resolution was negligibly small. However, from our more recent work we have determined that for the particular configuration used in the CBOOA experiments the longitudinal in-plane resolution function is better approximated by a Lorentzian rather than by a Gaussian function. Accordingly, we have now reanalyzed the data which formed the basis for this paper using a Lorentzian longitudinal in-plane resolution function. As we shall discuss below, this new data analysis leads to some modification of our conclusions.

Firstly, we find that the ratio of the longitudinal to transverse correlation lengths, $\xi_{\parallel}/\xi_{\perp}$, evolves from 5.5 ± 0.5 at $\tau \sim 10^{-2}$ to 8 ± 1 at $\tau \sim 10^{-4}$. This evolution, although very subtle, is clearly a real effect. We cannot, on the other hand, exclude the possibility that, for example, $\xi_{\parallel}/\xi_{\perp}$ is

constant for $\tau < 10^{-3}$ in CBOOA. The above increase in the length ratio by $\sim 45\%$ over two decades corresponds to an effective exponent difference $\nu_{\parallel} - \nu_{\perp} \sim 0.08$. We should emphasize, however, that one cannot infer from our experiments that $\xi_{\parallel}/\xi_{\perp}$ actually diverges at T_c ; that is, one cannot conclude that there are two fundamental lengths characterizing the *N-A* transition. Rather, one can only conclude that there is a subtle evolution in $\xi_{\parallel}/\xi_{\perp}$ down to 25 mK above T_c .

Secondly, our original data analysis gave the rather enigmatic result that the effective exponents seemed to exhibit a crossover from helium ($d=3$, $n=2$) to mean-field values as one approached T_c . This result is incorrect. For data analyzed with the correct resolution function we now find that all quantities exhibit a single power-law behavior over the complete temperature range measured $2 \times 10^{-2} \geq \tau \geq 8 \times 10^{-5}$. Explicitly, for the structure factor, and longitudinal and transverse correlation lengths, we find the exponents $\gamma = 1.30 \pm 0.06$, $\nu_{\parallel} = 0.70 \pm 0.04$, and $\nu_{\perp} = 0.62 \pm 0.04$, respectively, where the error limits are 2-standard-deviation statistical errors. We note that these are in satisfactory agreement with the $d=3$, $n=2$ values, $\gamma = 1.316$ and $\nu = 0.669$, thus lending strong support to de Gennes's helium-analog model for the *N-A* transition. The symmetric displacement of ν_{\parallel} and ν_{\perp} about the helium value is a very enticing feature of this data. It would be interesting to determine if the effective-length anisotropy mechanism suggested by Lubensky and Chen will account for this result.

A full report on this research together with related experiments in other biphenyl smectic liquid crystals will be published elsewhere.